The Rainbow Connection – Why Now is the Time for Smallsat Optical Downlinks

Doug Sinclair
Sinclair Interplanetary
dns@sinclairinterplanetary.com

Kathleen Riesing
Department of Aeronautics and Astronautics, Massachusetts Institute of Technology
kriesing@mit.edu

ABSTRACT

Many small satellite missions are data constrained, with payloads generating more data than can be sent to Earth over radio downlinks. To address this, we have developed a novel optical downlink system, comprising a space and ground terminal. The space terminal projects a 1 W laser beam with wavelength 785 nm, on-off modulated at 1 Gbps. It aims this at the ground station using a MEMS steering mirror, guided by an integral star tracker and rate sensors. The ground station is a 22" reflecting telescope with a fine steering mirror at the focal plane and a silicon avalanche photodiode detector. The use of a semiconductor tapered power amplifier, in place of a traditional doped fiber amplifier, makes this compact and low power. We believe this technology will allow even smaller spacecraft to carry data-intensive payloads.

INTRODUCTION

Space-borne sensors are of enormous utility to us as a society. They help us to forecast the weather, manage development and natural resources, and look out into the cosmos. Almost all of this data comes down to the ground via radio (RF).

For sensors with high data rates, the available bandwidth for RF can be a bottleneck. We can now envision small and inexpensive satellites that can carry sophisticated payloads, but which lack the budget and political clout to reserve a large Ku or Ka-band spectrum allocation.

We have set out to solve this need with optical downlinks. Our architecture includes a space terminal that will fit on a 10-kg class satellite, and a ground terminal no larger than the Yagi antennas typically used for RF tracking and commands. Together these deliver a 1 Gbps data link for a spacecraft in a 500 km LEO orbit.

While optical downlinks have been demonstrated on larger classes of spacecraft, only a few efforts have focused on optical communications for small platforms[1,2]. The approach presented here differs primarily in the selection of wavelength and in the design of a beaconless pointing and tracking system.

SYSTEM ARCHITECTURE

Table 1: Downlink Wavelength Comparison

λ (nm)	Pro	Con
785	• Good DC efficiency (TPA) • Small Tx aperture • Cheap Si guidance sensors • Wide RX FOV • Suitable for quantum key distribution	• Few COTS telecom parts available • Short range eye hazard • Little space heritage
1060	• Optical preamps available (very narrow RX FOV) • Good space heritage	• Expensive InGaAs guidance sensors • Narrow RX FOV • Short range eye hazard
1550	• Optical preamps available (very narrow RX FOV) • COTS telecom parts available • Eye safe • Good space heritage	• Poor DC efficiency (EDFA) • Large Tx aperture • Expensive InGaAs guidance sensors • Narrow RX FOV

Possibly the most important architectural decision for an optical downlink is its wavelength. We have chosen to use 785 nm, in the near-IR. This is unusual. Except for a few experiments with quantum cryptographic key distribution, most existing satellite optical links use short-wave IR at 1060 nm (primarily Europe) or 1550 nm (the rest of the world).

Those wavelengths are driven by the use of doped fiber amplifiers: 1060 nm for ytterbium and 1550 nm for erbium. In high performance systems doped fiber amplifiers are used in both the transmitters and receivers. Their prevalence in terrestrial fiber telecoms also ensures a wide selection of off-the-shelf components.

For a small satellite system with modest (<10 Gbps) data rates and pointing capabilities (< 10 arc-sec) these amplifiers are no longer necessary or even useful. Instead, we have chosen a system architecture with no doped fiber. This gives us a free choice of wavelength, unencumbered by the emission bands of particular rare-earth elements.

The 785 nm wavelength is short enough that we can use conventional silicon image sensors for tracking, and large area silicon Avalanche PhotoDiodes (APDs) for detection. It is long enough that it is invisible, and so the spacecraft does not become an unsightly distraction in the night sky. Finally, it has good transmission through the atmosphere.

Safety

Popular culture is full of examples of communications lasers becoming unintentional hazards[3] or even improvised weapons[4]. In designing the communications system we must make sure that they are demonstrably safe.

Table 2: Downlink Guidance Comparison

Guidance	Pro	Con
Stellar	• Completely eye safe • No interference/jamming • Star tracker useful for other functions	• Complex • Limited performance • Requires RF uplink & orbit knowledge
Beacon	• Simple • High performance • Can add uplink data	• Regulatory burden • Eye danger to aircraft • Vulnerable to interference/jamming

Traditional high-performance optical links use a beacon on the ground station to point up at the spacecraft. The spacecraft uses this as a reference for pointing its downlink beam, and can potentially achieve diffraction-limited performance. However there are safety concerns for aircraft passing through the beacon beam. These are generally addressed by restricting the air space over the ground station, and implementing a fail-safe shutdown using either radar or human spotters.

Restricting air traffic is impractical for a small satellite system that will have a small budget and potentially operate from many ground sites. By analysis it can be shown that some beacons do not present an eye hazard to cruising aircraft, but it is difficult to deal with the worst-case threat of the hovering helicopter pilot with binoculars[5]. We choose to design a ground station that is entirely passive, with no outgoing laser radiation. The space terminal points at the ground through a built-in star tracker, rather than an uplink beacon. Such a system is demonstrably safe.

The downlink is safe for viewers on the ground, or even astronauts on ISS, by virtue of the very large distance from the spacecraft to the observer. In order for the laser to exceed allowable limits an astronomer would have to look at it with a 10 meter class telescope – and no telescope that big has an eyepiece! With the naked eye a stargazer would receive roughly as many photons from the laser as from the planet Venus, which is clearly safe. Of course, the public perception remains to be seen..

Table 3: Link Budget

Laser Power (1 W)	0 dBW
Optical Losses	-0.50 dB
Photons per Joule	185.96 dB photons/J
Output Flux	185.46 dB photons/sec
Transmit Gain (0.01° x 0.06° beam)	77.83 dB
Pointing Loss	-3.00 dB
Free Space Loss (1000 km)	-130.99 dB/m^2
Atmospheric Loss	-2.00 dB
Receiver Power Density	127.3 dB photons/m^2/sec
Receiver Area (22" telescope)	-6.1 dB m^2
Optical Losses	-2.00 dB
Receive Flux	119.20 dB photons/sec
Uncoded Bit Rate (1 Gbps)	90.00 dB bits/sec
Photons per bit	29.20 dB photons/bit
OOK Sensitivity	20.41 dB photons/bit
Link Margin	8.79 dB

The link budget shows that a 1 W laser at 1000 km range can easily transfer 1 Gbps of data to a 22" class telescope. The downlink beam is large (0.01° x 0.06°) making the pointing problem less difficult. With

almost 1000 photons/bit at the receiver we can perform direct detection. We do not need sophisticated photon-counting receivers. Carrier phase is unimportant, so turbulence and adaptive optics are not concerns.
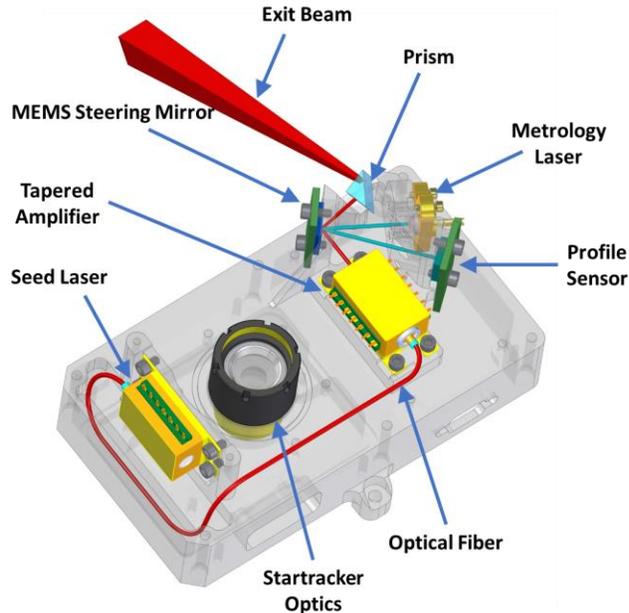
SPACE SEGMENT

Figure 1: Space Terminal Layout

The space terminal is built onto the reverse side of the optical bench of an expanded Sinclair Interplanetary ST-16RT2 star tracker. The entire package is 100 mm x 68 mm x 68 mm with a total mass of 415 g.

Referring to Figure 1, a seed laser provides the precise wavelength reference. It is intensity-modulated by the payload data, at a nominal rate of 1 Gbps, simply by controlling its drive current. The resulting signal has a power on the order of 10 mW.

A short length of optical fiber connects the seed laser to the Tapered Power Amplifier (TPA). The TPA is a solid-state semiconductor device that preserves the wavelength of the seed laser while boosting the power by a factor of 100. Collimating optics on the far end of the package launch a free-space beam, illustrated in red.

The beam bounces off a MEMS steering mirror and then a prism to target the ground station. A low-power visible pulsed laser (the metrology laser, shown in blue) also reflects off the MEMS steering mirror and onto a silicon profile sensor. This metrology system allows for realtime measurements of the mirror angle, which can then be controlled by adjusting the mirror actuator voltages.
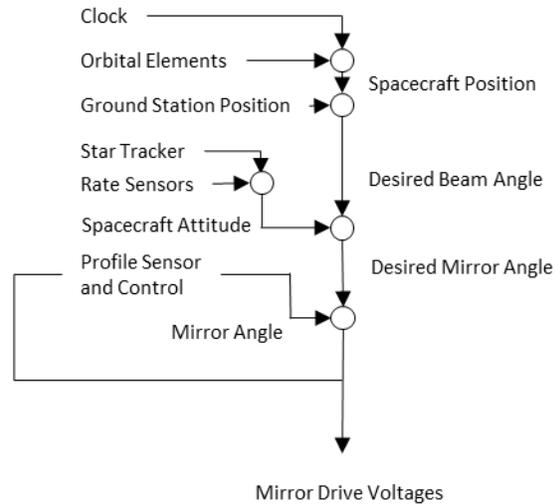

Figure 2: Space Pointing Loop

The star tracker boresight is nominally 125° from the output beam, which can be steered over a total of ±2° by the MEMS mirror. It is expected that the host spacecraft will coarsely point towards the ground station, and that the space terminal will then make fine corrections with the mirror. These maneuvers must be planned to respect the star tracker's Earth and sun exclusion zones.

With no uplink beacon to track, making sure the downlink beam reaches the ground station is not easy. To begin, we assume that the spacecraft knows its orbit and time. At 500 km altitude the beam footprint on the ground is an ellipse measuring 90 m x 520 m with its major axis aligned with the spacecraft velocity vector. The orbital location must be known to much better than this. Onboard GPS is one way to accomplish this.

Next, the space terminal establishes its attitude. The built-in star tracker provides absolute updates at 2 Hz (potentially 8 Hz with a software update). Built-in inertial rate sensors are used to extend the attitude knowledge to high frequency. Four three-axis MEMS sensors are used, with the data combined to reduce the overall noise.

Finally, the MEMS mirror is steered to point the downlink at the ground station. The metrology laser and profile sensor read the mirror angle at ~100 Hz allowing closed-loop control.

Pointing Results

The profile sensor is a 256 x 256 pixel array, subtending approximately 4° as seen by the MEMS mirror. Thus each pixel represents 0.016° of beam motion (making steep-angle reflection approximations).
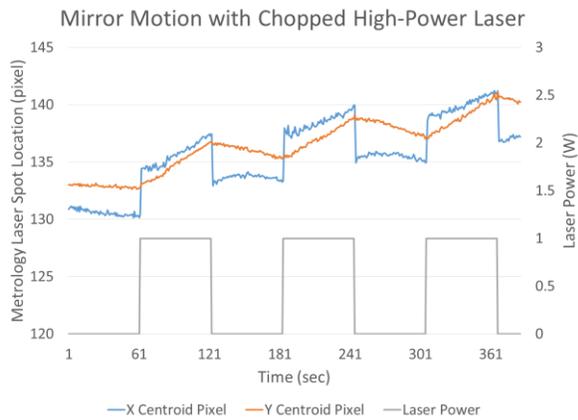
Figure 3: Open-Loop Mirror Motion

Figure 3 shows data from the profile sensor when the MEMS mirror drive voltages are held constant. The high-power laser is turned on and off with a 2-minute repeat time.

Both axes show a triangular waveform caused by heating. The magnitude is 7 pixels over the duration of the 6-minute test, giving a beam wander of 0.11°. In addition, the X-axis sees an instantaneous 4 pixel step upon application of the laser. We were surprised to trace this down to a photoelectric effect in a silicon flexure of the MEMS mirror which is illuminated by beam spill-over.
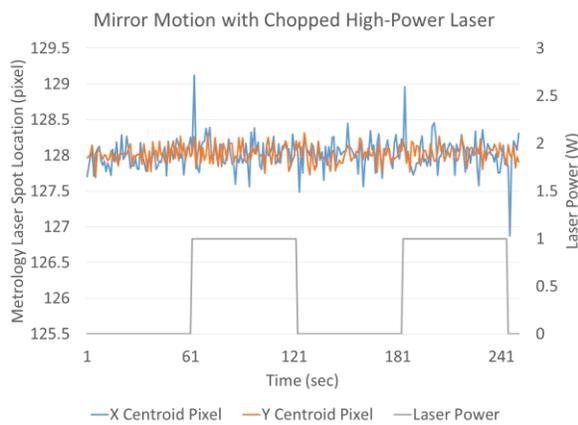

Figure 4: Closed-Loop Mirror Motion

Figure 4 shows data from a similar experiment. This time, the MEMS mirror drive voltages are directed to hold the metrology laser spot at the center of the profile sensor (pixel coordinates [128,128]). RMS error in the X axis is 0.21 pixels, corresponding to 0.0033°. The Y axis RMS error is 0.12 pixels, corresponding to 0.0019°. This level of performance is consistent with the pointing requirements.

Amplifier Results

Like the more familiar Doped Fiber Amplifiers (DFAs), TPAs are constant-power amplifiers. Both are typically fed with a constant power source. For a DFA, this is a pump laser with a wavelength shorter than the desired output. For a TPA, this is DC electric current. In each case, this input power raises atoms in the amplifier to an excited state. A photon from the seed laser passing by an excited atom will cause it to drop back into its base state while emitting an additional photon. The amplifier gain is effectively self-adjusting, making the average output power approximately constant over the long term.

The big difference between the DFA and the TPA is the time scale of energy storage. DFAs have time constants of milliseconds, which is sure to be slower than the modulation data rate. TPAs, however, have time constants shorter than a nanosecond.
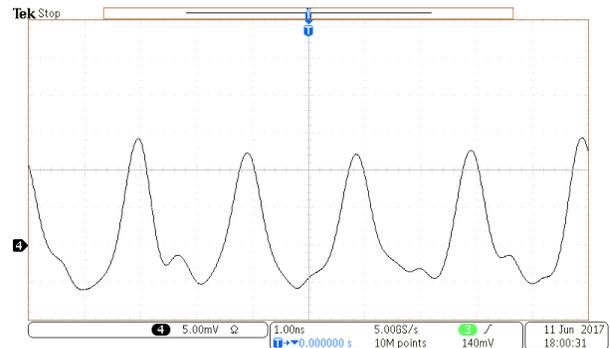

Figure 5: TPA Modulation with 01 Bit Pattern

Figure 5 shows the output of the TPA modulated with a 1 Gbps 0-1 digital pattern (equivalent to a 500 MHz square wave). This is close to the ideal output that we would hope for.
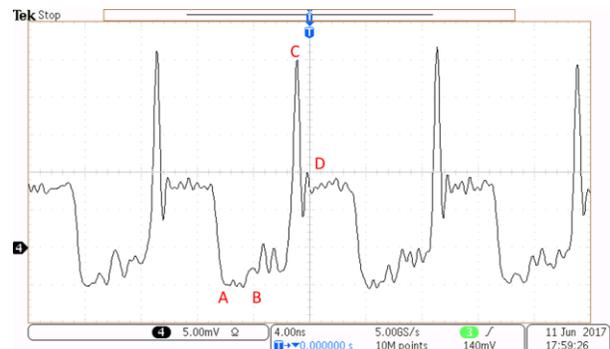

Figure 6: TPA Modulation with 0000011111 Bit Pattern

Figure 6 shows the same TPA, this time modulated with a pattern of five 0 bits followed by five 1 bits at 1 Gbps. This could also be thought of as a 01 pattern at 200 Mbps.

At moment A the seed laser has just turned off. The TPA has minimal stored energy, and has no output power. The DC current into the TPA is uninterrupted, and so energy starts to accumulate inside it.

Around point B, 1.5 ns after A, the TPA energy storage is full. Power starts to leak out in the form of Amplified Spontaneous Emission (ASE). The extinction ratio of the link is reduced, as we have optical radiation in a slot that should be a digital '0'.

At point C the seed laser turns on again. The TPA energy storage is full, so the gain is very high. There is a brief high-power pulse as the stored energy is consumed.

Finally, at point D the TPA has reached steady state. The optical power going out is balanced with the electrical power coming in.

This low-frequency behaviour of the TPA is undesirable, and forces us to high data rates. Even at 1 Gbps, some sort of coding is required to control the run length of 0 or 1 bits. Manchester coding is a simple way to accomplish this.

Efficiency

A standard Erbium Doped Fiber Amplifier (EDFA) operating at 1550 nm is fed by a semiconductor pump laser at 980 nm. This pump laser is not dissimilar in construction and efficiency to our 785 nm TPA. However an EDFA incorporates two sources of inefficiency. First, one pump photon at 980 nm can produce at most one signal photon at 1550 nm. This wastes a third of the pump power. Second, there is every possibility that a pump photon may be scattered or absorbed and not produce a signal photon. Put together, these factors give a 2x efficiency improvement for the TPA as compared to the EDFA.

The TPA (and the pump lasers in an EDFA) contain thermoelectric coolers to keep the semiconductor junctions at a controlled 25 °C. Surprisingly, the cooler will often consume more current than the junction. Both the cooler and the junction operate around 2-3 V, while the spacecraft power bus will be 12 V to 50 V (depending on its size and design). High efficiency step-down converters are key to good system efficiency.

We are experimenting with placing the TPA junction and cooler in series so that it appears as a single 6 V load to a step-down converter. A second two-quadrant converter at the mid-point, running in phase with the primary, tunes the current in both devices to maintain the desired temperature and output power.

Running at 28 V, our complete system consumes 10 W DC to generate 1 W of output laser power, run the coolers, drive and modulate the seed laser, and steer the MEMS mirror.

GROUND SEGMENT

The ground station is based around an amateur Dobsonian (i.e. altazimuth-mounted Newtonian) telescope (see Figure 7). We chose a 22" diameter primary (559 mm) as it is at the knee of the aperture-cost curve. We save little money going smaller, but would have to pay a lot to go larger.

Figure 7: Ground Station Telescope

The standard aluminum mirror coatings are unsuitable for use at 785 nm. We coated the primary mirror with protected gold, and the secondary with a 21-layer dielectric stack.

Ground station tracking (see Figure 8) can be split up into a coarse segment and a fine segment. The coarse segment consists of the telescope/mount with a coarse guidance camera mounted to the secondary support structure of the telescope. The guidance camera is co-boresighted with the telescope aperture with a 6° field-of-view. Its silicon detector can detect and match stars for telescope calibration, and can also directly detect the target spacecraft's downlink beam. This allows for very loose requirements on the open-loop tracking accuracy of the telescope.
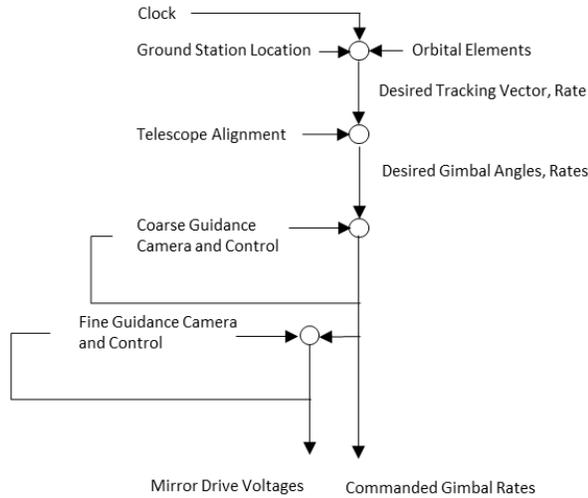
Figure 8: Ground Pointing Loop

Once the target is acquired in the coarse guidance camera, closed-loop feedback is used to improve the tracking of the telescope. The closed-loop accuracy of the coarse segment must be sufficient to handoff to the fine pointing segment which, after beam resizing, has a range of about 0.1°.

The fine segment (not shown in Figure 7) consists of collimating optics, a fast steering mirror, and a beam splitter that divides the signal between a fine guidance camera and an APD receiver. 10% of the light goes to the camera, and 90% goes to a silicon APD.

Table 4: Ground Station Pointing Requirement

Telescope focal length	2300 mm
APD diameter	0.5 mm
Instantaneous FOV	0.0126°

We want to use the largest possible APD to simplify the pointing requirements on the telescope. However, large APDs have limited bandwidth. With a cutoff frequency of 1 GHz we are limited to devices having a diameter of approximately 0.5 mm.

Combined with the focal length of the telescope, this APD diameter gives a FOV of 0.0126° (~45 arcsec). So long as the fast steering mirror can deliver this performance, the APD will catch all of the incident photons. Both the ground and space segment end up with roughly equivalent pointing requirements.

The output of the APD is fed into a commercial demodulator IC. We have demonstrated clock and data recovery at up to 1 Gbps.

CONCLUSION

We believe that optical downlinks are feasible for small spacecraft. We do not do this by shrinking a traditional big spacecraft link, but by designing a new architecture.

Instead of short-wave IR at 1550 nm, we use near IR at 785 nm. This lets us use a physically large silicon APD at the ground station, which relaxes the telescope pointing requirement.

Instead of an uplink beacon, we use a star tracker on the space terminal. This makes the ground station safe, and removes all need for us to coordinate with air traffic. The star tracker provides additional benefits for spacecraft payload pointing.

Instead of high-performance phase-modulation, we use simple on-off intensity-modulation. This means that we have no sensitivity to wavefront error. We can use large telescopes, sited at low-altitude locations, without requiring adaptive optics.

If events unfold as we hope, we will have space-terminals on-orbit and ground terminals installed by the end of 2017, and will be able to verify our performance.

REFERENCES

1. Janson, Siegfried and Richard Welle, "The NASA Optical Communication and Sensor Demonstration Program: An Update," Proceedings of the 28th Annual AIAA/USU Conference on Small Satellites, 2014.

2. E. Clements et al., "Nanosatellite optical downlink experiment: design, simulation, and prototyping," Opt. Eng., vol. 55, no. 11, 2016.

3. Carpenter, John, "Dark Star", Bryanston Pictures, 1974.

4. Niven, Larry, "The Warriors", If (magazine), February 1966.

5. "Eye Safety Constraints for 1.06 μm and 1.55 μm Free Space Optical Communications", CNES, 2012.